Search for 2S-state metastability in muonic helium at 40 atm

M. Eckhause, P. Guss, D. Joyce, J. R. Kane, R. T. Siegel, W. Vulcan, R. E. Welsh, and R. Whyley
College of William and Mary, Williamsburg, Virginia 23185

R. Dietlicher and A. Zehnder
Swiss Institute for Nuclear Research, 5234 Villigen, Switzerland
(Received 18 July 1985)

A search was made for photons from the two-photon deexcitation of the 2S state of muonic He by measuring the time and energy distributions of delayed photons emitted when negative muons were stopped in gaseous He at room temperature. An upper limit of 46±1 ns was obtained for the lifetime of this state at 40 atm, in disagreement with earlier measurements. Prompt K-series muonic x rays were also measured at pressures between 0.5 and 40 atm, and the x-ray intensity ratios were used to deduce initial 2S-state populations.

I. INTRODUCTION

The muonic He ion, consisting of a negative muon bound to a helium nucleus, has been studied experimentally for many years at CERN,[1-4] where emphasis has been on the measurement of the 2S-2P splittings as a test of quantum electrodynamics[5-7] (QED). The 2S state has also been of interest because of proposed studies of weak-neutral-current (WNC) effects.[8,9] The CERN QED experiments and the prospect for WNC experiments both depend on the metastability of the muonic He 2S state, which in contrast to atomic hydrogen lies below the 2P state, as is true[8] for muonic ions with $Z<3$. The muonic helium ion has thus far been the only low-Z muonic ion reported to evidence metastability of the 2S state despite searches involving various other targets.[10-12]

The 2S metastability in the muonic He ion was studied at CERN by Placci, Carboni, Bertin, and co-workers[1-4] by observation of one or both photons from the 2γ deexcitation from the 2S to the 1S state, this being the dominant radiative deexcitation mode, with a predicted[8,9,13] rate $\lambda_{2\gamma}=1.181\times10^5/\text{s}$. The photons from this process are well known to display a spectrum of approximately semicircular character beginning at zero energy and ending at the 2S-1S transition energy, which in muonic He lies only about 1 eV below the 8224-eV 2P-1S transition energy. The two photons from the 2γ process must have energies which sum to the 2S-1S energy.

The proposed experiments on WNC involving muonic ions would require that the mixing of 2S and 2P states induced by collisions of the ion with neighboring atoms occur at a rate comparable to or smaller than the deexcitation rate of the 2S state to the 1S ground state by single M1 photon emission ($\frac{1}{2}$ s^{-1}). At CERN, it was found that in He at 30–50 atm the collisional Stark mixing rate was $\lambda_{\text{St}}<300\ [P(\text{atm})]\text{s}^{-1}$. It follows that if this effect is linear with pressure, then at a few Torr it might be sufficiently small to permit WNC experiments, assuming a sufficiently intense source of stopped muons can be constructed. It was the purpose of the present experiment to measure the total collisional deexcitation rate λ_c, which includes λ_{St} as well as other possible deexcitation processes, over a range of pressures sufficient to (a) verify the CERN result for λ_{St} and (b) test the dependence of λ_c on pressure.

It is to be noted that the theoretical Stark quenching rate for the 2S state is substantially greater than that measured at CERN, as has been discussed in detail by Cohen,[14] who found the theoretical expectation for quenching in two-body collisions to be 1.4×10^5 $\text{s}^{-1}\text{atm}^{-1}$. Even if simple molecular ions involving the muonic helium ion and neighboring helium atoms are quickly formed, Cohen[14] calculated that zero-point motion of the muonic ion should then produce quenching within $<10^{-7}$ s. Such molecular ions are indeed expected to form rapidly (<1 ns) at the pressures used in Refs. 1–4. Thus a mechanism was hypothesized by which the Stark quenching rate is reduced by cluster formation, whereby an approximately spherical distribution of helium atoms forms about the muonic ion and protects it from Stark quenching in collisions. As we have noted, Cohen's calculations are not consistent with this hypothesis.

Shortly before the present experiment was performed von Arb *et al.*, at the Swiss Institute for Nuclear Research (SIN), using gas scintillation proportional counters, observed the single and double photons from the 2γ $2S\rightarrow1S$ deexcitation of muonic helium ions formed at pressures well below 1 atm.[15] von Arb *et al.* also observed that this deexcitation mode, which served as evidence for the presence of the 2S state, was quenched quadratically at pressures between 100 and 600 Torr, as Cohen had predicted. At 6 atm von Arb *et al.*[15] did not observe any two-photon deexcitation, being able only to set a limit on this mode which was substantially below the level reported by Placci *et al.*[1] at 7 atm. These SIN results make the original CERN observations[1-4] even more puzzling, since the latter can be explained only if a new phenomenon arises at yet higher pressures to provide the evidence for delayed two-photon emission reported in the CERN work at 7–50 atm.

II. DESCRIPTION OF THE EXPERIMENT

The experimental apparatus is shown schematically in Fig. 1 and consisted of a target pressure vessel assembly tested to 60 atm, a gas handling system, a beam-defining counter telescope, two detectors for 3—20-keV photons, and an electronic logic and data acquisition system. The target assembly was placed in the $\mu E4$ beam at SIN, with the nominal momentum of the negative muon beam set at 39 MeV/c. A 2.2-cm-diam collimator defined the beam as it entered the target vessel. For each gas pressure used in the target, the beam transport system magnet currents were adjusted to optimize the number of muons stopping in the central region of the 10-cm-long, 1-liter-volume gas target.

Counters S1 and S2 were (20×24)-cm^2 thin (0.6 mm) plastic scintillators. Counter S3 was a 190-μm-thick $\times4.5$-cm^2 Si surface barrier detector located inside the gas target volume, and counter S4 was an aluminized 63-mm-thick scintillation cup located inside the target vessel. The aluminized coating served to suppress outgassing of the plastic scintillant which might contaminate the target gas. S4 covered all except the front surface of the target volume and was viewed through a rear 5-cm-thick Lucite window by two photomultipliers. In addition to detecting those beam particles which pass through the target gas, S4 was also used to detect electrons from muons decaying within the target volume.

The photon detectors were high-resolution [200-eV full width at half maximum (FWHM) at 5.9 keV] Si(Li) detectors 300 mm$^2\times5$-mm deep which viewed the target gas volume through 46-mm-diam holes cut through S4 and also through 1.70-mm-thick Be windows mounted in the side walls of the stainless-steel target vessel.

Because of concern about possible contamination of the target He gas by impurities emanating from various surfaces exposed to the gas, precautions were taken to limit

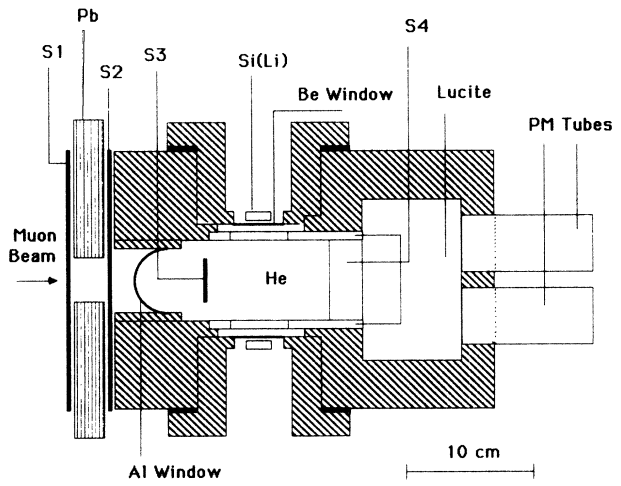

FIG. 1. Schematic plan view of apparatus. S1, S2, S4, scintillation counters; S3, Si surface barrier detector. PM tubes view S4 through the Lucite pressure window via ports in the end plate. The body of the target vessel (diagonal shading) is of stainless steel.

and monitor such contamination. All accessible surfaces inside the target system were cleaned with Freon before and after assembly in order to remove residual organic contaminants. After assembly, both the target system and the gas circulation system (see below) were heated with external coils and evacuated continuously for a two-week period. (The target vessel itself was not heated, since this would damage the counter S4 inside.) A residual gas analyzer used to monitor the gas purity during this period showed the impurity level of $A<100$ gases to be less than 0.1 ppm when the target vessel was finally filled to a pressure of 40 atm.

When the target was filled, the gas in the system was circulated by a pump at a rate of about 1 liter per minute, independent of the target pressure. The circulation was through a system of filters and purifier elements, the most important of which were an oven filled with titanium turnings heated to 600 °C followed by a trap filled with zeolite and cooled to liquid-nitrogen temperature. Samples of the circulating gas were taken periodically for later analysis. Such analysis by a commercial laboratory showed water vapor, O_2, N_2, and other impurities below the sensitivity limits of the measuring techniques, about 1 ppm for each component other than He.

Possible deexcitation mechanisms of the $(\mu\mathrm{He})^+$ ions in collisions with impurities necessitated particular attention to maintaining target gas purity. For example, the muonic ion, which acts in atomic collisions much like a free proton, could exchange with a proton in an H_2O molecule and become bound in that molecule.[15,16] If the muonic ion were in a metastable $2S$ state before such an exchange collision, it would be expected to deexcite rapidly once bound in the water molecule. The purification techniques used in this experiment were expected to remove contaminants to a level of 10^{-8}, a value low enough to prevent such quenching mechanisms from affecting the experimental results.

Charged particles were detected by counters S1—S4. The times of flight between S1 (or S2) and S4 prior to filling the target with gas were sufficiently different for electrons and muons in the beam to enable us to distinguish the two kinds of particles. Thus it was possible to set S1 and S2 discriminator levels so as to distinguish muons from beam electrons having the same momentum. The linear signals from S1 and S2 were then each fanned out to two discriminators, one of which was set low (L) to accept all beam particles and the other of which was set to a higher (H) level to accept only beam muons. The electronic logic system then processed these signals with those from other counters to produce combinations ("labels") which were then used to open or close gates, identify various event types, exclude background, etc. The functions of the logic system can be summarized as follows in terms of the labels.

(a) Identify beam particles which are incident upon the target vessel but do not enter it. The label was for the prompt coincidence and anticoincidence combination $\mathrm{S1_L}\cdot\mathrm{S2_L}\cdot\underline{\mathrm{S3}}\equiv\underline{\mathrm{MISS}}$, which was used to trigger a 0.4-μs gate within which all events were rejected.

(b) Identify all beam particles entering the target volume. The label was $\mathrm{S1_L}\cdot\mathrm{S2_L}\cdot\mathrm{S3}\equiv\underline{\mathrm{BEAM}}$, which was used

primarily to suppress events associated with the occurrence of more than one beam particle entering the target volume within a 10-μs gate.

(c) Identify muons stopping within the gas target volume. The label was $S1_H \cdot S2_H \cdot S3 \cdot \underline{S4} \equiv \underline{\text{MUON}}$, which was used to trigger all events.

(d) Form a 10-μs gated coincidence between stopped muons (MUON) and events in either photon detector (PHOTON). The label was MUON·PHOTON≡FASTSLOW, and events of this type were sorted according to whether a decay electron was also detected within the 10-μs gate. They also were "cleaned" of possible backgrounds as described in (a) and (b).

(e) Reject FASTSLOW events in which the photon followed the decay electron. Such events were labeled as BADPHOTON.

(f) Reject events occurring during dead time of the data acquisition logic and on-line computer. The blanking signal from such origins was labeled BUSYMONITOR and was typically activated less than 3% of the time.

(g) Accumulate a sample of PHOTON and MUON signals occurring out of coincidence for off-line study of background.

(h) For each accepted FASTSLOW event [cf. (d) above], digitize the detection time relative to MUON and also the energy deposited in each counter, the relevant photon detector, and the electron counter $S4$.

(i) Generate an event trigger along with an event-type identification for storing each accepted event on magnetic tape, and for on-line analysis of a portion of the events in order to monitor performance of the system.

Figure 2 is a simplified block diagram of the electronic logic system for the experiment.

III. ANALYSIS OF THE DATA

A. Time distribution of events

The search for $2S$-state metastability involved analysis of events in which a muon stop was followed first by a photon of energy no greater than 8.2 keV and then by a decay electron, both occurring within 10 μs of the muon stop. The time interval explored for delayed photons started at $\approx$200 ns before the centroid of the muon stop time distribution and included the full 10 μs following that centroid. Time resolution was better than 55-ns FWHM (Fig. 3). The time region explored allowed analysis of random background after several muon lifetimes had elapsed, and a further exploration of possible backgrounds was facilitated by extending the energy region for the recording of photons from 0 to 20 keV. Thus background photons in the K-series region from 8.2 to 12.4 keV and above could be studied and, as will be seen below, were significant in the interpretation of the data.

The recording of both the time and the energy for the delayed photons and also for the subsequent electron permitted a multidimensional analysis of the events accepted by the electronic logic system. As a first step in the analysis we studied the time distribution for electrons which followed photons occurring in the prompt time peak around the muon stop signal. These electrons

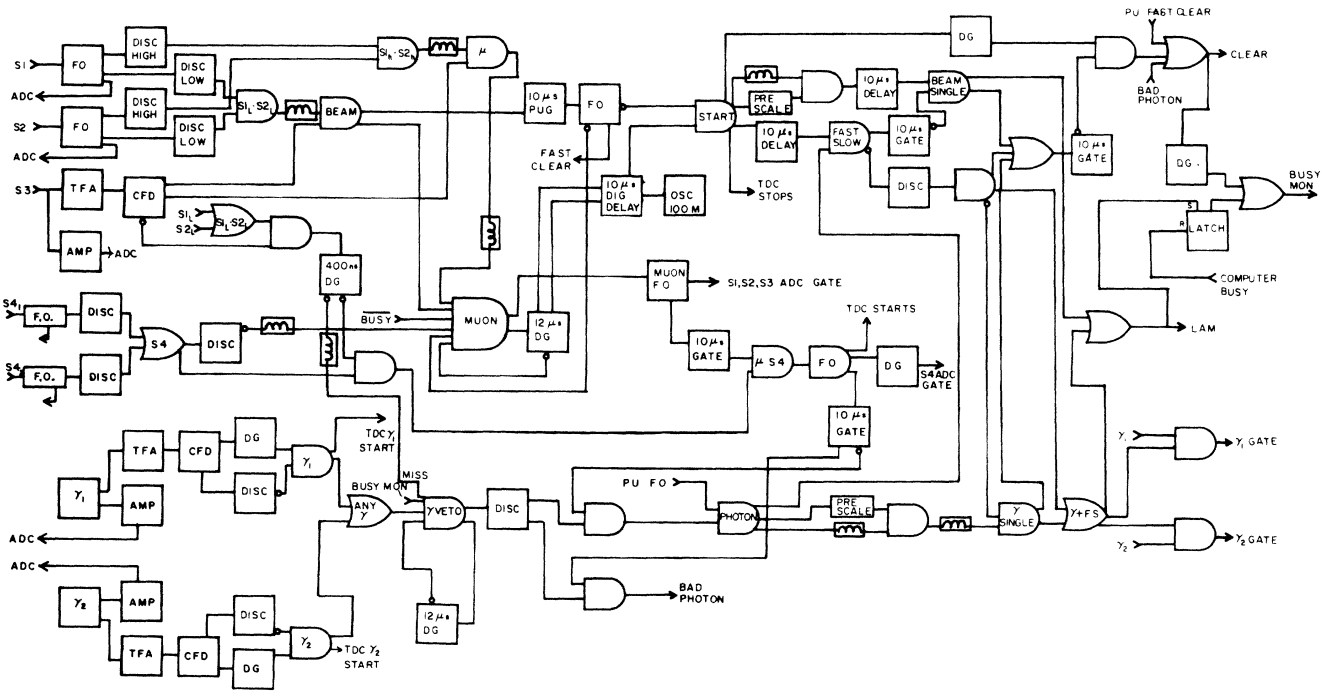

FIG. 2. Simplified block diagram of the electronic logic.

display the usual exponential decay time spectrum for negative muons (Fig. 4), with little background.

Next, the time distribution was studied for events in which a photon occurring up to 10 μs following the muon stop was in turn succeeded by an event in the electron counter. The electron time accepted also extended to 10 μs after the muon stop. The photons in this analysis were in energy region I, extending from 0 to 8.2 keV. If such photons are from the two-photon deexcitation of muonic helium ions, the succeeding electron time distributions should exhibit the usual exponential plus background characteristic of muon decay, and the photon time distribution should have the exponential character of the total $2S$-state disappearance rate along with a possible background component. (The energy spectrum of the photons should be appropriate to the two-photon spectrum from the $2S$ state.) The doubly differential probability of detecting a delayed photon in the time interval dt_γ and a subsequent electron in the interval dt_e is in fact proportional to $P(t_\gamma)P(t_e)dt_\gamma dt_e$, where

$$(1)\quad P(t_\gamma)=\exp[-(\lambda_{b\gamma}+\lambda_{be})t_\gamma][\lambda_{b\gamma}(1-\epsilon_e\{1-\exp[-(\lambda_0+\lambda_{be})t_\gamma]\})+\epsilon_{2S}\lambda_{2\gamma}\exp(-\lambda_t t_\gamma)]\ ,$$

$$(2)\quad P(t_e)=\exp[-\lambda_{be}(t_e-t_\gamma)][\lambda_{be}(1-\epsilon_e\{\exp[-(\lambda_0+\lambda_{be})t_\gamma]-\exp[-(\lambda_0+\lambda_{be})t_e]\})+\epsilon_e\lambda_0\exp[-\lambda_0(t_e-t_\gamma)]]\ .$$

Here t_γ and t_e are the photon and electron times measured from the muon stop signal; $\lambda_{b\gamma}$ and λ_{be} are the accidental background rates in the photon and electron detectors, respectively; ϵ_e is the efficiency of the electron detector, including solid angle factor; ϵ_{2S} is the efficiency for detecting the photon from two-photon decay of the $2S$ state (including the $2S$ population factor for each stopped muon, the detector solid angle factor, and the Be window transmission factor); λ_0 is the muon disappearance rate from the $1S$ state; $\lambda_{2\gamma}$ is the two-photon deexcitation rate of the $2S$ state; and λ_t is the total disappearance rate of the $2S$ state, which includes both λ_0 and $\lambda_{2\gamma}$ as well as the collisional deexcitation rates λ_c, i.e., $\lambda_t=\lambda_0+\lambda_{2\gamma}+\lambda_c$. (The nuclear capture rate for muons in the $1S$ or $2S$ states is negligible compared to all other rates in the expression above and has been ignored.) There was also an amplitude factor applied to this distribution for normalization purposes. The efficiencies ϵ_{2S} and ϵ_e were obtained by Monte Carlo calculations; ϵ_{2S} included an initial population for the $2S$ state which was deduced from measured prompt x-ray intensity ratios (cf. Sec. IV below).

We applied the method of maximum likelihood to find

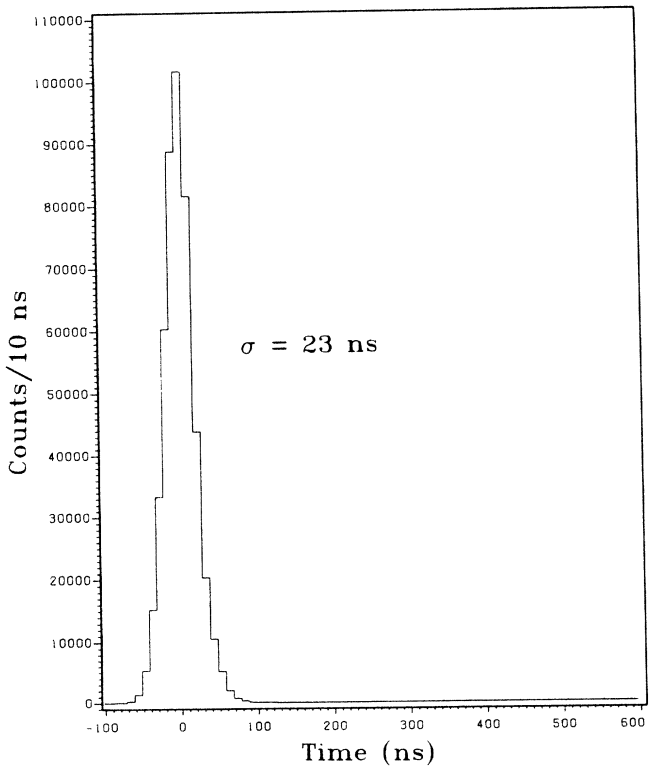

FIG. 3. Time distribution of the 8.2–12.4-keV photons (muonic He K-series region) in coincidence with S1·S2·S3·S4. These are *prompt* photons. Background is included, but is too small to be visible on this scale.

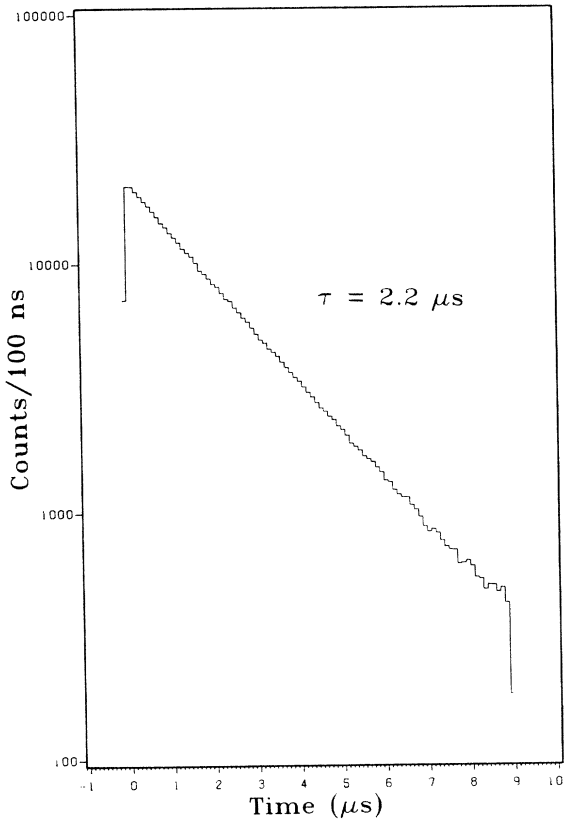

FIG. 4. Time distribution of S4 (electron) signals following *prompt* photons in one Si(Li) detector. Background is included. The slope is that of the negative muon lifetime in He.

experimental values for the free parameters in the above expression. The likelihood function was that for Poisson statistics:[17]

$$L_p(y,n)=\prod \exp(-y_{ij}/n_{ij}) ,$$

where the product is taken over all i and j. Here i labels the ith t_γ time bin and j labels jth t_e time bin, and n_{ij} represents the experimental number of counts in the bin ij. The y_{ij} represents the value obtained from the fitting function, which was obtained by standard procedures for linearization.[17] The errors which we report below correspond to one standard deviation.

The parameter of greatest interest is λ_c, which includes the effects of all collisional processes which deplete the muonic $2S$ state. We therefore undertook to analyze the timing data assuming accepted values for λ_0 and $\lambda_{2\gamma}$ and Monte Carlo values for the efficiencies ϵ_{2S} and ϵ_e for 2γ-photon and electron detection. The analysis was performed via the program MINUIT (Ref. 18) and included timing data for γe events starting with those in which the photon occurred in the prompt peak, i.e., coincident with the stopping muon, and including photons delayed up to 10 μs. For this analysis the prompt photon timing peak was convoluted with the expression for $P(t_\gamma)$ in the first equation above. There is some uncertainty in the exact form of the prompt photon timing peak, which is dominantly of Gaussian form but may have non-Gaussian wings because of the Si(Li) detector characteristics at the energies involved. Thus the analysis yields a result for λ_c which must be regarded as a lower limit for that parameter. The analysis yielded $\lambda_c = 21.6 \pm 0.4$ MHz. This value dominates other contributions to the total disappearance rate λ_t of the $2S$ muonic He state at 40 atm and leads to a lifetime for that state of $\tau_{2S} \equiv 1/\lambda_t < 46 \pm 1$ ns. Quoted errors on these results for λ_c and τ_{2S} are statistical standard deviations.

Another analysis of the data involving photons in energy region I was performed involving *all* delayed events in a photon detector followed by a signal from the electron counter. In this analysis an electron count was accepted only if it occurred within a fixed period of 2 μs after detection of the photon. Events of this description were called "γe-TC" events. The rate of such γe-TC events *per muon stop* was measured for five different incident beam rates. Clearly, γe-TC events which originate with a single stopping muon, as would be the case for events from metastable $2S$ muonic He, would show a yield per stopping muon independent of beam rate. Figure 5 shows the results of this test for events in energy region I (below 8 keV) indicating an approximately linear increase of delayed γe-TC events with increasing beam intensity. Most of the events recorded thus appear to be accidental coincidences between a delayed photon in a Si(Li) detector and a signal in the electron counter. Assuming maximum metastability of the $2S$ state, i.e., setting $\lambda_c \equiv 0$, the residual γe-TC event rate extrapolated to zero muon intensity corresponds (at 40 atm) to an initial population for the $2S$ state of $(3.13 \pm 1.92) \times 10^{-3}$, which is not in agreement with the value ($\approx 7 \times 10^{-2}$) resulting from prompt x-ray intensity measurements to be described below. This result is consistent with the time analysis results above in the sense that both indicate an absence of evidence for the metastability of the $2S$ state in muonic He, in disagreement with the CERN results[1-4] at similar pressures.

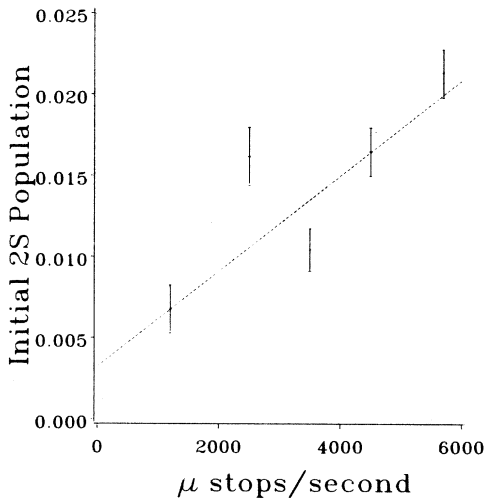

FIG. 5. Initial $2S$-state population, assuming metastability, as deduced from the "γe-TC" event rate vs muon stop rate. (See text.) The dotted line is a linear least-squares fit to the data.

B. Photon energy spectra

The two high-resolution Si(Li) photon detectors which viewed the target volume were calibrated with various radioactive sources for linearity of response versus energy. A characteristic energy spectrum of x rays which were in prompt time coincidence with the muon stop signal with 40 atm of high-purity He in the target is shown in Fig. 6. The K series from muonic He dominates, with the $K\alpha$ peak well resolved from $K\beta$ and higher members of the series. Small background peaks which appear at 6.4 keV and near 13 keV, attributed to muonic Be $L\alpha$ and muonic C $L\alpha$, respectively,[19] are probably the result of muon stops in the Be windows and in the scintillation plastic.

Figure 7 displays a characteristic energy spectrum of photons which comprised the events in which a *delayed* photon was followed by a signal in the electron counter. The K-series peaks are clearly visible, and the 6.4-keV peak is also identified. At first glance it is surprising that the K series, which is associated with the stopping of the muons, should also appear in the delayed events. However, the intensity of the *delayed* K-series peaks is about 5×10^{-4} of the prompt K-series intensity. It is not unlikely that such a fraction of second incoming muons should fail to be registered in the incident counter circuitry and thus give rise to the K-series x-ray peaks in the delayed spectrum of Fig. 7.

With the exception of the peaks in Fig. 7 already mentioned, the spectrum appears to have no distinct features. The Be window transmission factor suppresses the low-energy portion of the spectrum. At higher energies the residual spectrum (neglecting the peaks) declines smoothly. Such behavior is characteristic of many possible background spectra, such as that from bremsstrahlung by de-

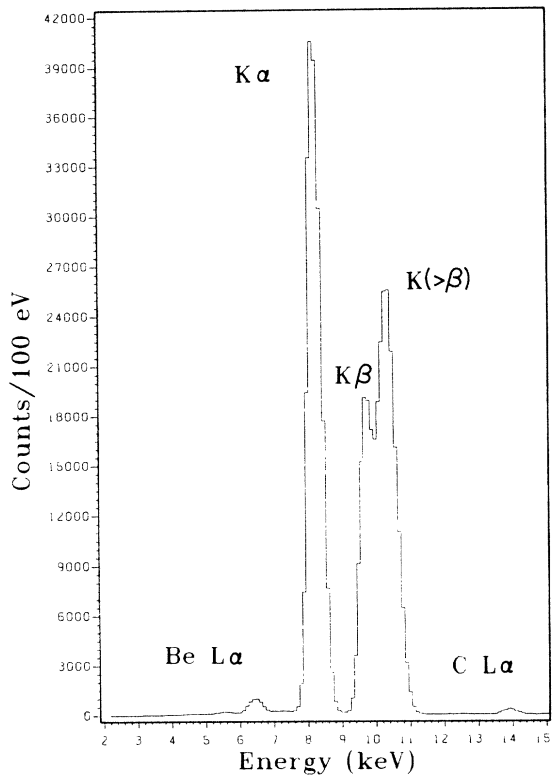

FIG. 6. Energy spectrum of *prompt* photons (cf. Fig. 3). All background is shown in the figure.

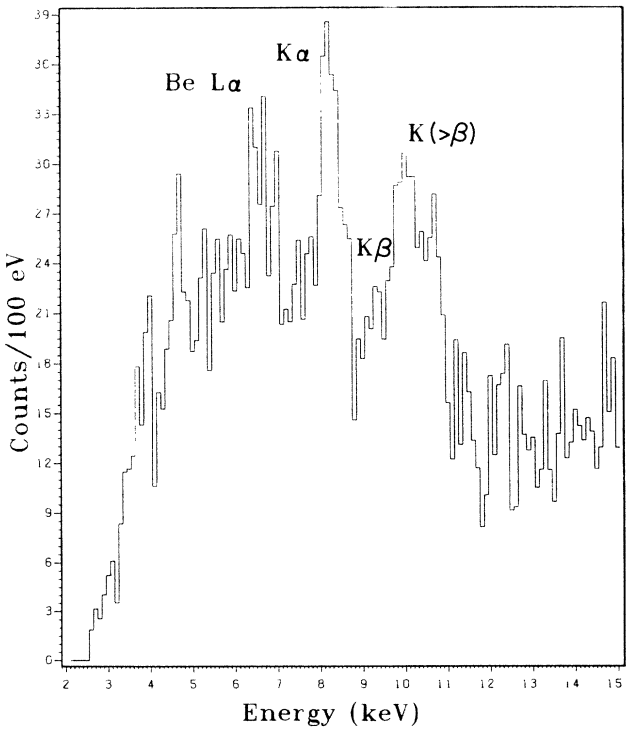

FIG. 7. Energy spectrum of *delayed* photons each associated with an electron (S4) signal within 0.2—10 μs of the muon stop signal initiating the event. All background is shown in the figure. See text.

cay electrons in the Be windows or other material of the target chamber near the windows. We thus do not find evidence in Fig. 7 for two-photon decay of the $2S$ state of muonic He.

C. Intensities of the K-series muonic He x rays

The initial population of the $2S$ state in muonic helium was deduced from the observed intensities of the *prompt* K-series x rays, i.e., those coincident with stopping muons. The absolute detection efficiencies for the various members of the K series were not required for this purpose, but the *variation* in efficiencies through the K series had to be measured. This was accomplished by a preliminary test in which γ rays from test sources were transmitted through one of the Be windows later used in the target. The transmission experiment was performed in good geometry, and the results compared well with the values predicted from the chemical analyses of the material from which the Be windows (which contained significant impurities) were fabricated and a recent tabulation of photon mass attenuation coefficients.[20] The stopping muons were distributed in a finite region of the target, so that the geometry of the transmission test was an imperfect simulation of the actual experimental conditions, but since only the variation in transmission from 8 to 12 keV was needed, the error introduced was small. The prompt muonic x-ray spectra from negative muons stopping in He at room temperature and at seven different pressures were analyzed as follows. Such events were defined as comprising first a muon stop signal with an accompanying x ray within ± 50 ns of the centroid of the time distribution of signals from the photon detector relative to muon stops and also a signal from the electron counter within 10 μs of the muon stop signal. The relative yields of prompt muonic K-series x rays thus selected were analyzed by a χ^2 minimization technique. For prompt photon events with energies between 4 and 14 keV, histograms of the observed events versus energy were fitted to a spectrum consisting of Gaussian peaks at the known[21] positions for K-series x rays in muonic He, plus a background declining exponentially with increasing energy. The transitions producing $K(>\delta)$ were assumed to yield a single Gaussian peak. In addition, resolution (FWHM) of each peak was fixed from calibration with radioactive sources, leaving only the amplitude of each Gaussian and the parameters of the background free to vary in the analysis.

X-ray histograms corresponding to gas pressure of 0.5, 5.0, 10.0, 20.0, 30.0, 35.0, and 40.0 atm were analyzed in this manner. The yield of each Gaussian x-ray peak was then corrected for the transmission of the Be windows as described above and relative yields obtained for the various x rays.

Table I gives the relative K-series x-ray yields at the pressures measured during this experiment. The quoted errors are statistical only. These measured intensity ratios were then used to calculate the "initial" $2S$-state population E_{2S}, i.e., the population at the end of the muon's cascade through the atomic levels to either the $1S$ state or the

TABLE I. K-series x-ray intensity ratios for muonic He from 0.5 to 40 atm.

Pressure (atm)	$K\alpha/K_{\text{tot}}$	$K\beta/K_{\text{tot}}$	$K\gamma/K_{\text{tot}}$	$K\delta/K_{\text{tot}}$	$K(>\delta)/K_{\text{tot}}$
0.5	0.662±0.055	0.110±0.012	0.035±0.011	0.023±0.025	0.170±0.073
5.0	0.556±0.016	0.102±0.004	0.079±0.005	0.102±0.010	0.161±0.023
10.0	0.507±0.016	0.117±0.005	0.105±0.006	0.136±0.011	0.134±0.024
20.0	0.484±0.011	0.141±0.004	0.151±0.005	0.122±0.009	0.103±0.017
30.0	0.489±0.008	0.165±0.004	0.184±0.005	0.090±0.007	0.072±0.014
35.0	0.479±0.008	0.183±0.003	0.183±0.004	0.090±0.006	0.065±0.011
40.0	0.482±0.002	0.198±0.001	0.206±0.002	0.061±0.001	0.054±0.001

$2S$ state, the only two levels from which deexcitation by single $E1$ photons cannot occur in muonic He.

The calculation was based on the method of Bertin *et al.*,[4] who had used their $K\alpha/K_{\text{tot}}$ intensity ratio measurement at a given pressure to place bounds on E_{2S} at that pressure. We extended their method to include the effects of all K-series ratios available from our measurements, namely $K\alpha$, $K\beta$, $K\gamma$, $K\delta$, and $K(>\delta)$. The notation is wherever possible identical to that of Ref. 4. Define

$$F(n,1)=\frac{\Gamma_{nP-1S}}{\Gamma_{nP-2S}}=\frac{1}{8}\frac{(n-1)^{2n-3}(n+2)^{2n+3}}{(n+1)^{2n+3}(n-2)^{2n-3}}$$

as the ratio of the radiative transition probabilities $\Gamma_{nP\text{-}1S}$ and $\Gamma_{nP\text{-}2S}$. $F_{\text{av}}(n,1)$ is then defined as the average value of $F(n,1)$ over all bound states higher than n through which the muon cascades, i.e., all higher states up to $n\approx 14$. The uncertainty assigned to $F_{\text{av}}(n,1)$ was $\{\pm[F(n,1)-F(14,1)]/2\}$. We also define

$$d_{mn}=[1/F(m,1)-1/F_{\text{av}}(n,1)] .$$

We consider the population E_{2S} for two of the cases described in Ref. 4. For the first (case A), the $2S$ state is metastable, so that the prompt K-series x-ray ratios directly yield the value of E_{2S} for case A, which we call E^A_{2S} below:

$$E^A_{2S}=1-K_{\text{tot}}=K\beta/F(3,1)+K\gamma/F(4,1)+K\delta/F(5,1)+K(>\delta)/F_{\text{av}}(6,1) .$$

Let

$$N=1-K\alpha/K_{\text{tot}}+(K\beta/K_{\text{tot}})d_{36}F_{\text{av}}(6,1)+(K\gamma/K_{\text{tot}})d_{46}F_{\text{av}}(6,1)+(K\delta/K_{\text{tot}})d_{56}F_{\text{av}}(6,1) .$$

Then

$$E^A_{2S}=N/[N+F_{\text{av}}(6,1)] .$$

If the prompt x-ray spectra are such that the ratios $K\alpha/K_{\text{tot}}$ through $K\delta/K_{\text{tot}}$ and also $K(>\delta)/K_{\text{tot}}$ can be measured, the above expression gives the $2S$ population if that state is metastable.

We also consider the situation (case B) in which the ambient electric fields, either in the medium if in condensed state or due to collisions in a gas target, are sufficiently intense to mix thoroughly $2S$ and $2P$ states in a time short compared to the resolution of the experimental apparatus. In this completely Stark-mixed case, the observed K ratios still give information on the initial $2S$ population, which can be calculated by extension of the methods of Ref. 4 to obtain

$$E^B_{2S}=(1-K\alpha/K_{\text{tot}})/F_{\text{av}}(6,1)+(K\beta/K_{\text{tot}})d_{36}+(K\gamma/K_{\text{tot}})d_{46}+(K\delta/K_{\text{tot}})d_{56} .$$

We did not consider the other case dealt with in Ref. 4, that in which the external Auger effect during the muonic cascade occurs at a rate sufficient to affect the initial $2S$ population. The experimental information of external Auger rates is scanty,[2] and *a priori* calculations are also limited.[22]

Table II exhibits the results for $2S$ initial populations deduced from our K x-ray measurements with the above formulas. Errors quoted for case A were propagated from Table I, and case B entries have the same errors as corresponding entries for case A. These errors are considerably reduced from those in earlier work[1–4,15] because of the inclusion of the higher K-series transition ratios (cf. Table I). At each pressure, the populations for case B are higher than those for case A, i.e., Stark mixing appears to increase the initial $2S$ population rather than to deplete it, as already expressed in Ref. 4, where the effect was noted in muonic hydrogen. Our results for the $2S$ population are consistently higher in muonic He than those of the earlier CERN work[1–4]—the superior resolution of the Si(Li) detectors developed in the intervening years made possible the more precise results reported here. Our results at 0.5 and 5.0 atm are consistent with the results of von Arb *et al.*[15] at 400 and 600 Torr and 6 atm.

TABLE II. "Initial" $2S$ populations in muonic He, calculated from data in Table I. See text for definitions of case A and case B.

Pressure (atm)	E^A_{2S} (case A)	E^B_{2S} (case B)
0.5	0.0448±0.008	0.0478
5.0	0.0593±0.003	0.0630
10.0	0.0653±0.003	0.0698
20.0	0.0678±0.003	0.0727
30.0	0.0669±0.003	0.0717
35.0	0.0680±0.002	0.0729
40.0	0.0686±0.002	0.0723

IV. SUMMARY AND CONCLUSIONS

The results quoted above do not confirm earlier evidence[1-4] for metastability lifetimes of the order of 1 μs for the $2S$ state of the muonic He ion in 40-atm He at room temperature. The time analysis of Sec. II indicates a collisionally limited lifetime for this state of $<(46\pm1)$ ns under these conditions, compared to (1.8 ± 0.4) μs quoted in Ref. 1 at 7 atm and (1.43 ± 0.15) μs in Ref. 3 at 50 atm. In the present experiment the analysis of delayed γe events with the electron following the photon within 2 μs showed that most such events were accidental. Precautions taken in this work to achieve and maintain adequate gas purity appear to be at least comparable to those reported in the CERN experiments.

The absence of metastability at 40 atm appears to be consistent with the results of von Arb *et al.*[15] in that the $2S$ quenching observed by them below 600 Torr showed a quadratic pressure dependence. Continuation of that behavior at higher pressures would lead to a metastability lifetime at 40 atm well below the limits of sensitivity of the present experiment.

The K-series x-ray intensity ratios for muonic He indicate an initial $2S$-state formation rate which slowly rises from about 5% to 7% as the pressure increases from 0.5 to 40 atm. The intensity ratios are in smooth continuation of the results of Ref. 15.

ACKNOWLEDGMENTS

We acknowledge the contributions of R. D. Hart and A. Brodie to the early phases of the experiment. This work was supported in part by the U.S. National Science Foundation and by the Swiss Institute for Nuclear Research (SIN). We also thank the staff of SIN for its assistance during the experiment.

[1] A. Placci *et al.*, Nuovo Cimento **1A**, 445 (1971).
[2] G. Carboni *et al.*, Lett. Nuovo Cimento **6**, 233 (1973).
[3] A. Bertin *et al.*, Phys. Rev. Lett. **33**, 253 (1974).
[4] A. Bertin *et al.*, Nuovo Cimento **26B**, 433 (1975); A. Bertin, A. Vacchi, and A. Vitale, Lett. Nuovo Cimento **18**, 277 (1977).
[5] A. Bertin *et al.*, Nuovo Cimento **23B**, 489 (1974).
[6] A. Bertin *et al.*, Phys. Lett. **55B**, 411 (1975).
[7] G. Carboni *et al.*, Phys. Lett. **73B**, 229 (1978).
[8] J. Bernabeu, T. E. O. Ericson, and C. Jarlskog, Phys. Lett. **50B**, 467 (1974).
[9] G. Feinberg and M. Y. Chen, Phys. Rev. D **10**, 190 (1974).
[10] P. O. Egan *et al.*, Phys. Rev. A **23**, 1152 (1981).
[11] H. Anderhub *et al.*, Phys. Lett. **71B**, 443 (1977).
[12] A. L. Carter *et al.*, Phys. Lett. **124B**. 465 (1983).
[13] J. Shapiro and G. Breit, Phys. Rev. **113**, 179 (1959); R. Bacher, Z. Phys. A **315**, 135 (1984) gives the value quoted here.
[14] J. S. Cohen, Phys. Rev. A **25**, 1791 (1982).
[15] H. P. von Arb *et al.*, Phys. Lett. **136B**, 232 (1984).
[16] H. P. von Arb *et al.* (unpublished).
[17] P. R. Bevington, *Data Reduction and Error Analysis for the Physical Sciences* (McGraw-Hill, New York, 1969), p. 232ff.
[18] F. James and M. Roos, Comput. Phys. Commun. **10**, 343 (1975).
[19] T. von Egidy and H. Povel, Nucl. Phys. **A232**, 511 (1974); W. W. Sapp, thesis, College of William and Mary, 1970.
[20] J. H. Hubbell, Int. J. Appl. Radiat. Isot. **33**, 1269 (1982).
[21] G. Backenstoss *et al.*, Nucl. Phys. **A232**, 519 (1974).
[22] R. Landua and E. Klempt, Phys. Rev. Lett. **48**, 1722 (1982).